



The polarity protein Par6 is coupled to the microtubule network during molluscan early embryogenesis

Taihei Homma^a, Miho Shimizu^b, Reiko Kuroda^{a,b,c,*}

^a Department of Biophysics and Biochemistry, Graduate School of Science, The University of Tokyo, Hongo, Bunkyo-ku, Tokyo 113-0033, Japan

^b Kuroda Chiromorphology Team, ERATO-SORST, JST, Komaba, Meguro-ku, Tokyo 153-8902, Japan

^c Department of Life Sciences, Graduate School of Arts and Sciences, The University of Tokyo, Komaba, Meguro-ku, Tokyo 153-8902, Japan

ARTICLE INFO

Article history:

Received 16 November 2010

Available online 25 November 2010

Keywords:

Par6

Microtubules

Embryogenesis

ABSTRACT

Cell polarity, which directs the orientation of asymmetric cell division and segregation of fate determinants, is a fundamental feature of development and differentiation. Regulators of polarity have been extensively studied, and the critical importance of the Par (partitioning-defective) complex as the polarity machinery is now recognized in a wide range of eukaryotic systems. The Par polarity module is evolutionarily conserved, but its mechanism and cooperating factors vary among different systems. Here we describe the cloning and characterization of a pond snail *Lymnaea stagnalis* homologue of *partitioning-defective 6* (*Lspar6*). The protein product LsPar6 shows high affinity for microtubules and localizes to the mitotic apparatus during embryonic cell division. *In vitro* assays revealed direct binding of LsPar6 to tubulin and microtubules, which is the first evidence of the direct interaction between the two proteins. The interaction is mediated by two distinct regions of LsPar6 both located in the N-terminal half. Atypical PKC, a functional partner of Par6, was also found to localize to the mitotic spindle. These results suggest that the *L. stagnalis* Par complex employs the microtubule network in cell polarity processes during the early embryogenesis. Identical sequence and localization of LsPar6 for the dextral and the sinistral snails exclude the possibility of the gene being the primary determinant of handedness.

© 2010 Elsevier Inc. All rights reserved.

1. Introduction

Cell asymmetry and polarity are of fundamental importance to the animal body plan [1]. In the development of gastropods (snails), embryonic asymmetry introduced into the early blastomere configuration defines the patterns of later gene expression and developmental fates [2]. The asymmetry is generated by a conserved cleavage pattern (known as spiral cleavage), which is characterized by alternating blastomere rotation in clockwise and counter-clockwise directions [3]. Chirality (left–right) choice in this cleavage is generally fixed within a species by a single gene locus and manifests the body handedness (e.g., the direction of shell coiling) of the future adult snail [2,4,5]. The gene(s) regulating this asymmetry remains to be identified, but is suggested to be a modulator of the cytoskeleton in the case of *Lymnaea stagnalis* [6,7]. The snail *L. stagnalis* comes in both dextral and sinistral forms in nature

and provides a unique system for studying the origin of organismal chirality. Our previous studies revealed that the blastomere rotation in spiral cleavage involves directionally polarized cellular dynamics [7]. At the third cleavage, genetically dominant dextral embryos exhibit dextro-helical cell deformation and associated spindle inclination, which are both absent in recessive sinistral embryos. We have been focusing on this cellular dynamics and isolated *L. stagnalis* gene homologues known to regulate cell morphology and spindle dynamics in other organisms.

Par polarity proteins have been reported to be regulators of polarized cytoskeletal reorganization, including actomyosin dynamics [8,9] and the mitotic spindle reorientation [10]. A typical Par protein complex contains Par3, Par6, and atypical PKC (aPKC), with Par3 and Par6 being the scaffold proteins and aPKC functioning as a protein kinase [11,12]. Par proteins are also well-known regulators of body axis formation [13,14]. Bergmann and colleagues have reported the involvement of three par genes (*par-3*, *-4*, and *-6*) in handedness choice of early *Caenorhabditis elegans* embryos [15]. Thus, we searched for *L. stagnalis* par gene homologues to study their possible involvement in chirality establishment processes using both the dextral and sinistral snail lines. Herein we report the gene cloning of *L. stagnalis* Par6 and its tight association with the microtubule cytoskeleton. Although several studies have

Abbreviations: LsPar6, *Lymnaea stagnalis* partitioning-defective 6; aPKC, atypical protein kinase C.

* Corresponding author at: Department of Life Sciences, Graduate School of Arts and Sciences, The University of Tokyo, Komaba, Meguro-ku, Tokyo 153-8902, Japan. Fax: +81 3 5454 6600.

E-mail address: ckuroda@mail.ecc.u-tokyo.ac.jp (R. Kuroda).

shown the localization of Par6 on microtubule structures [16,17], this is the first report that demonstrates the direct interaction between Par6 and microtubules.

2. Materials and methods

2.1. Animals

L. stagnalis used in this study was described in [18]. Immunofluorescence and biochemical assays were performed using either both of the dextral and sinistral snail lines or only the dextral snail line (if chirality is not described).

2.2. Cloning

A set of degenerate primers was designed based on a conserved amino acid sequence of the PDZ domains of vertebrates and *Drosophila* Par6. Using the primers, a 200 bp RT-PCR product was amplified from total RNA isolated from the hermaphrodite duct of *L. stagnalis*. This was followed by 5' and 3' rapid amplification of cDNA ends (RACE) using the SMART-RACE kit (Clontech) to complete the full sequence. For the cloning of *L. stagnalis* aPKC, degenerate primers were prepared based on a conserved sequence within the catalytic domains of aPKCs. The degenerate primers used were 5'-CCIYTIGGITYTAYATHMG-3' and 5'-CATCATRTCIGTIA CYTGRTC-3' for Par6 and 5'-AARYTICIGARGARCA YGC-3' and 5'-IC CIGCCATCATYTCRAACAT-3' for aPKC.

2.3. Antibodies and reagents

Anti-Par6 antibody was raised in rabbit against a peptide corresponding to amino acids 85–104 of *L. stagnalis* Par6 and affinity-purified (Sigma–Genosys). The following antibodies were obtained from commercial sources: mouse anti- β -tubulin (clone TUB2.1; Sigma), anti-GST (clone 4C10; Covance), anti-Ran (clone 20; BD Transduction Laboratories), and rabbit anti-PKC ζ (C-20; Santa Cruz). Taxol and nocodazole were purchased from Sigma and dissolved in DMSO as stock solutions.

2.4. Immunofluorescence

Embryos were fixed at room temperature for 1 h in a fixative containing 1% paraformaldehyde, 0.15% glutaraldehyde, and 0.1% Triton X-100 buffered with PHEM (30 mM PIPES/12.5 mM HEPES/2.5 mM EGTA/1 mM MgCl₂, pH 6.9). Free aldehydes were reduced with NaBH₄. Fixed embryos were permeabilized with Triton X-100 (0.3%) and blocked with 5% normal goat serum before incubation with primary antibodies. Antibodies were diluted in PBS supplemented with 0.1% Tween 20 and 1–2% goat serum. Labeled embryos were visualized and photographed using a Zeiss LSM 5 PASCAL confocal microscope under a 20 \times objective lens. All images are single optical sections.

2.5. Inhibitor treatment

To depolymerize microtubules, embryos in prometaphase were treated with 200 nM nocodazole at room temperature for 20 min. Treated and control (vehicle: 0.02% DMSO) embryos were fixed, labeled, and observed as described above.

2.6. Expression and purification of recombinant proteins

Full-length and fragments of LsPar6 were amplified by PCR from gonad cDNAs and subcloned into pGEX-4T-3. Primers used for amplification of full-length LsPar6 were 5'-CGGGATCCATGTC AAGA

AGTTC AAGGG-3' and 5'-CCGCTCGAGTTAGAGTGTGACAGTTGG-3'. Plasmids were transformed into *Escherichia coli* DH5 α for sequencing and then into BL21 for protein expression. After induction with isopropyl β -D-thiogalactoside (IPTG), bacteria were harvested by centrifugation and resuspended in sonication buffer [20 mM Tris–HCl (pH 7.4), 150 mM NaCl, 2 mM DTT, and 1 \times Complete protease inhibitor cocktail (Roche)]. The cells were lysed by sonication (Handy Sonic sonicator UR-20P; Tomy Seiko), followed by the addition of 1% Triton X-100. Fusion protein purification was carried out using GST Purification Module (GE healthcare). Purified proteins were eluted with 20 mM reduced glutathione and dialyzed overnight at 4 °C against 20 mM HEPES (pH 7.0) and 150 mM NaCl. The dialyzed proteins were concentrated (Microcon; Millipore) and stored in 30% glycerol at –70 °C. The GST pulldown assay was performed at 4 °C in PHEM buffer plus 150 mM NaCl. Before each assay, the recombinant proteins were centrifuged to remove potential aggregates.

2.7. Microtubule cosedimentation assay

Embryos were collected after nuclear envelope breakdown and lysed at room temperature in lysis buffer (0.5% Triton X-100, 25 mM NaF, 0.5 mM Na₃VO₄, 1 mM DTT, and 1 \times Complete protease inhibitor cocktail in PHEM buffer). Endogenous microtubules were polymerized and stabilized by the addition of 0.5 mM GTP and taxol (20 μ M final). Stabilized microtubules were sedimented through 30% sucrose cushion by centrifugation at 50,000g (Beckman TLA100 rotor) for 30 min at 22 °C. For cosedimentation with exogenous microtubules, lysates were prepared on ice and clarified by pre-centrifugation. The lysates were then warmed to room temperature and supplemented with taxol-stabilized bovine microtubules (0.2 mg/ml, final). Either 4 mM Mg-AMP-PNP or 4 mM Mg-ATP was added with the exogenous microtubules. The mixture was incubated for 30 min at room temperature before centrifugation. For the cosedimentation assay with GST-fusion proteins, recombinant proteins were mixed at room temperature with taxol-stabilized microtubules (0.6 mg/ml, final) in PHEM buffer plus 150 mM NaCl, and centrifuged at 100,000g for 30 min through 40% sucrose cushion. All results are representative of at least three independent experiments.

2.8. Immunoblotting

Protein samples were separated on SDS–PAGE and blotted onto Hybond-P membrane (Amersham). The blots were challenged with antibodies and developed using the ECL advance kit (GE healthcare). HRP-anti-mouse and anti-rabbit IgG (GE healthcare) were used at 1:140,000 and 1:150,000 dilution, respectively. For evaluation of antibody specificity, an antibody mixture was preincubated with the corresponding antigen peptide (1:200 M ratio) at room temperature for 1 h and then applied to the blocked membrane.

2.9. Microtubule bundling assay

X-rhodamine labeled tubulin was purchased from Cytoskeleton and reconstituted according to the manufacturer's instructions. Polymerized and taxol-stabilized microtubules were mixed with protein samples or storage buffer [10 mM HEPES (pH 7.0), 75 mM NaCl, and 30% glycerol] and incubated at room temperature for 10 min. The final concentration of tubulin was 4 μ M (0.4 mg/ml). The reactions were fixed with 1% glutaraldehyde, diluted and mounted with 60% glycerol, and observed with the LSM 5 confocal microscope.

3. Results and discussion

3.1. Characterization of *L. stagnalis* Par6

A full-length cDNA encoding *L. stagnalis* Par6 was isolated using degenerate PCR and 5' and 3' RACE. The full-length cDNA sequence has been deposited in DDBJ (ID: AB598832). The identical sequence was obtained from both the dextral and sinistral *L. stagnalis* strains. LsPar6 contains the conserved PB1 domain, the half-CRIB motif, and the PDZ domain, displaying about 45% amino acid sequence identity with vertebrate Par6 and 47% identity with *Drosophila* Par6 (Fig. S1). The phosphorylatable serine (threonine) residue close to the C-terminus, which is present in vertebrate Par6 homologues, is also conserved in *L. stagnalis*. This residue is a target for TGF- β -mediated phosphorylation in vertebrates and indicates the linkage between Par6 and the tight-junctional pathway [19].

We examined the cellular localization of LsPar6 in early embryos using an antibody raised against the N-terminal sequence of LsPar6 (Fig. 1). Antibody specificity was confirmed by immunoblotting and a peptide competition assay (Fig. 1A). In mitotic embryos, the antibody gave a filamentous staining pattern which resembles the microtubular structure (Fig. 1B). In the M-phase, immunoreactivity was observed in the whole mitotic apparatus including the centrosome, the mitotic spindle and astral microtubules. This pattern was observed at all stages examined from 1-cell to trochophore (data not shown). In G2 phase embryos, the antibody labeled the peri-centrosomal region and centrosomal microtubules. The microtubular staining observed in the G2 and M phases were dispersed throughout the cytoplasm in the S-phase, except for that remained at the spindle midzone/midbody. Neither cortical nor junctional localization, as observed in other organisms, was detected by this antibody.

3.2. LsPar6 localization on microtubules and its implication to the snail chirality

LsPar6 localization on microtubules was confirmed by double immunofluorescence with an anti-tubulin antibody (Fig. 2). The filamentous pattern of LsPar6 was coaligned with that of microtu-

bules (Fig. 2A). This localization was suppressed when treated with the microtubule-disrupting agent nocodazole ($n = 26/26$; Fig. S2), while the actin filament-disrupting agent Latrunculin A had no effect on the colocalization (data not shown).

We compared the LsPar6 staining pattern between the dextral and sinistral handedness embryos (dextral and sinistral embryos are shown in Fig. 2A and B, respectively). Although the fluorescence intensity is weak in the sinistral embryos (probably due to the different permeability of the fixed embryo), there is virtually no difference in the LsPar6 staining pattern for the dextral and sinistral embryos. Thus, together with the result of amino acid consistency, LsPar6 is less likely the primary determinant of the snail body handedness. On the other hand, the mitotic spindle with LsPar6 on its microtubules undergoes enantio-directed relocation and reorientation during the spiral cleavage, and so does the axis of the polarity protein distribution. Therefore, LsPar6 may function not in the creation but rather in the establishment or fixation of the polarity which is generated by the handedness-determining gene.

3.3. LsPar6 directly interacts with microtubules and possesses the *in vitro* microtubule bundling ability

To assess the microtubule-binding ability of LsPar6, we performed a microtubule-cosedimentation assay. Microtubules in mitotic embryo extracts were stabilized with the aid of taxol and GTP. Stabilized microtubules were centrifuged, and proteins in the pellet fraction were analyzed by SDS-PAGE and immunoblotting. LsPar6 was detected in the pellet fraction together with endogenous microtubules, while most of the control protein Ran was found in the supernatant (Fig. 3A). Similar cosedimentation was observed with exogenous (bovine) microtubules supplemented to the lysates (Fig. 3B). Neither ATP nor AMP-PNP affected the cosedimentation, suggesting that LsPar6 binds microtubules directly or through a nucleotide-insensitive adapter protein(s).

We then evaluated the ability of LsPar6 to interact directly with microtubules and tubulin. The full-length and truncation mutants of LsPar6 fused to glutathione S-transferase (GST) were prepared (Fig. 3C) for *in vitro* binding assays. The full-length LsPar6 was found to bind to tubulin in the GST-pulldown assay (Fig. 3D). The

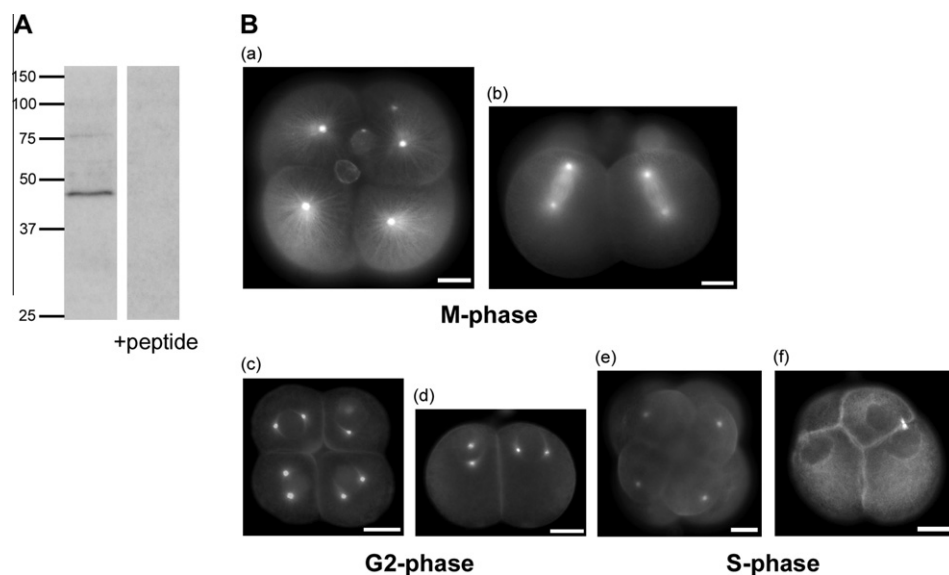
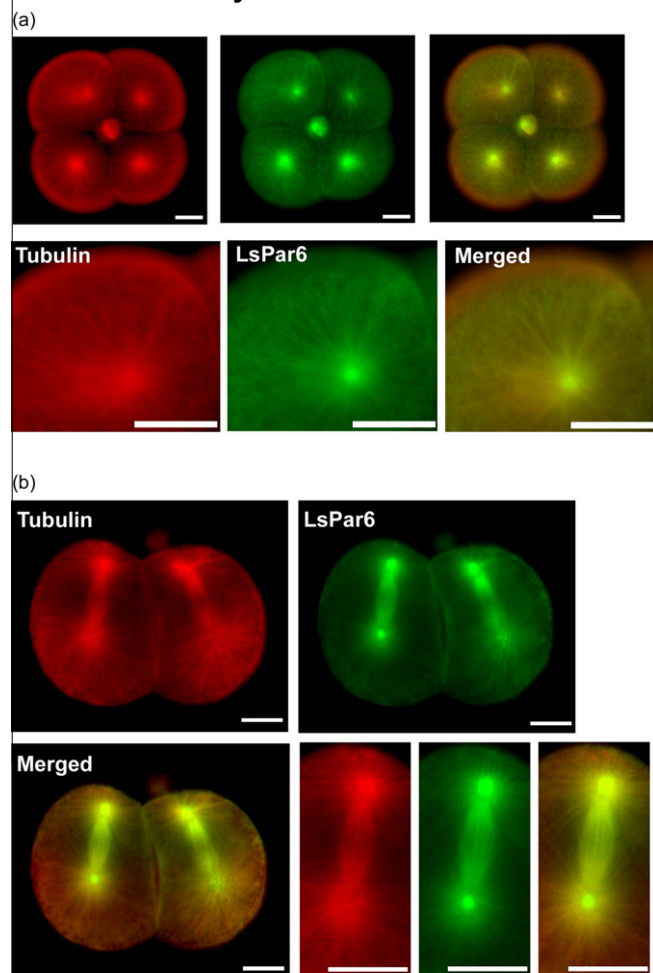


Fig. 1. Characterization of LsPar6. (A) Immunoblotting with anti-LsPar6 antibody. Extracts were prepared from embryos at 4-cell stage. Anti-LsPar6 antibody detected a single band which migrated near its predicted molecular weight of 42.5 kDa (left). The band disappeared when the antibody was preadsorbed with the immunizing peptide (right). (B) Immunofluorescence. Embryos at the third cleavage (4- to 8-cell stage) were fixed, and labeled with anti-LsPar6 antibody, followed by FITC-conjugated secondary antibody. Immunoreactivity was detected along the microtubular structure, with an intense signal in the centrosomal region (M and G2 phases). In the S-phase, the antibody labeled the spindle midbody. (a–d) 4-Cell stage, animal view (a, c) and side view (b, d); (e, f) 8-cell stage, animal view (e) and side view (f). Bars represent 20 μ m.

A Dextral embryos



B Sinistral embryos

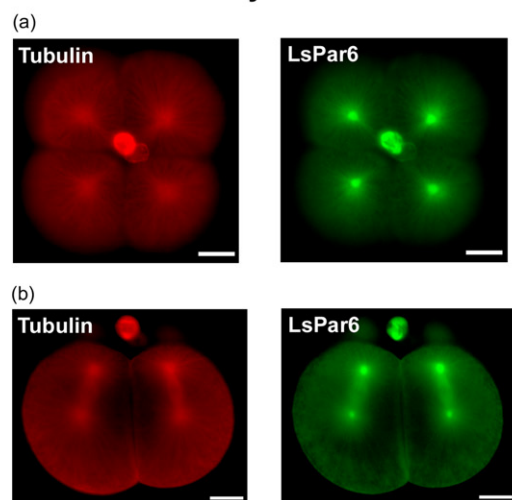


Fig. 2. LsPar6 localizes to the mitotic apparatus. (A) Double immunofluorescence of LsPar6 and microtubules. Embryos of the dextral strain were simultaneously stained for β -tubulin (red) and LsPar6 (green) and merged. Merged images show a coalignment of LsPar6 and the microtubule filament. (a) 4-Cell stage, animal view; (b) 4-cell stage, side view. Bars represent 20 μ m. (B) Immunofluorescence on the sinistral embryos. Embryos of the sinistral strain were immunolabeled as in A. The same microtubule structures were observed in both the dextral and sinistral embryos. (a) 4-Cell stage, animal view; (b) 4-cell stage side view. Bars represent 20 μ m. (For interpretation of the references in colour in this figure legend, the reader is referred to the web version of this article.)

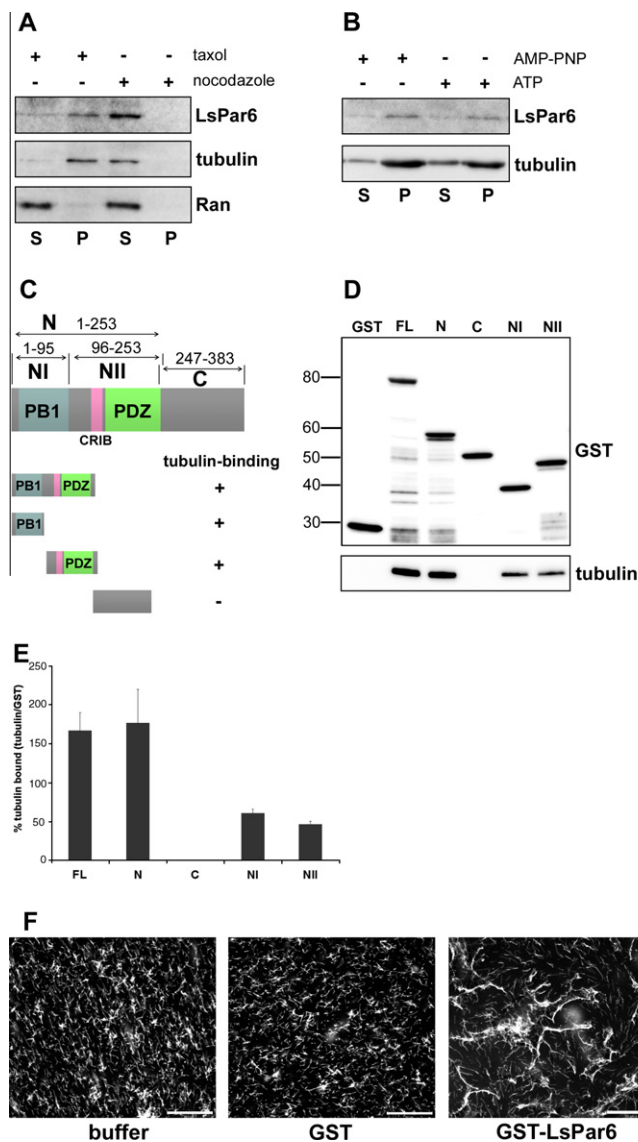


Fig. 3. LsPar6 interacts with tubulin and microtubules. (A) Cosedimentation assay with endogenous microtubules. Microtubules in mitotic embryo extracts were either stabilized or disrupted by the addition of taxol (20 μ M) or nocodazole (200 nM), respectively. Par6 was sedimented only in the presence of stabilized microtubules. The nuclear protein Ran serves as a negative control for cosedimentation. S, supernatant; P, pellet. (B) Cosedimentation assay with exogenous microtubules. Microtubules were reconstituted with exogenously supplied bovine tubulin. Either AMP-PNP or ATP was added to the reactions in order to assess the nucleotide-sensitivity of the cosedimentation. (C) Schematic diagram of GST-fused LsPar6 proteins used in the binding assays. GST was fused to the N terminus of full-length LsPar6 or each truncation mutants of LsPar6 (N: 1–253, C: 247–383, NI: 1–95, NII: 96–253). (D) GST-pulldown assay. Equal amount (molar basis) of each GST-fused protein was incubated with 0.5 μ M of bovine tubulin, and then precipitated with GSH-Sepharose beads. The recovered proteins were analyzed by SDS-PAGE and immunoblotting. (E) Quantification of bound tubulin in the pulldown assay. Band intensity was quantified using Image Gauge software (FUJIFILM). The intensity of each tubulin band was normalized to the corresponding GST-protein level. Data represent average values with standard deviations ($n = 3$). (F) Microtubule-bundling assay. X-rhodamine tubulin was polymerized into microtubules with taxol, and then mixed with either buffer, 5 μ M GST, or 5 μ M GST-LsPar6. The mixtures were incubated for 10 min at room temperature, fixed, and analyzed under the confocal microscope (40 \times objective). Images are representatives of at least 10 fields from three independent experiments. Bars represent 50 μ m.

binding ability resides in the N-terminal half of LsPar6 (amino acid 1–253), within which we have found two non-overlapping interaction regions (NI; 1–95, and NII; 96–253). NI contains the PB1 domain, while NII possesses the half-CRIB and the PDZ domain. Each of the motif and domains has interacting protein partners

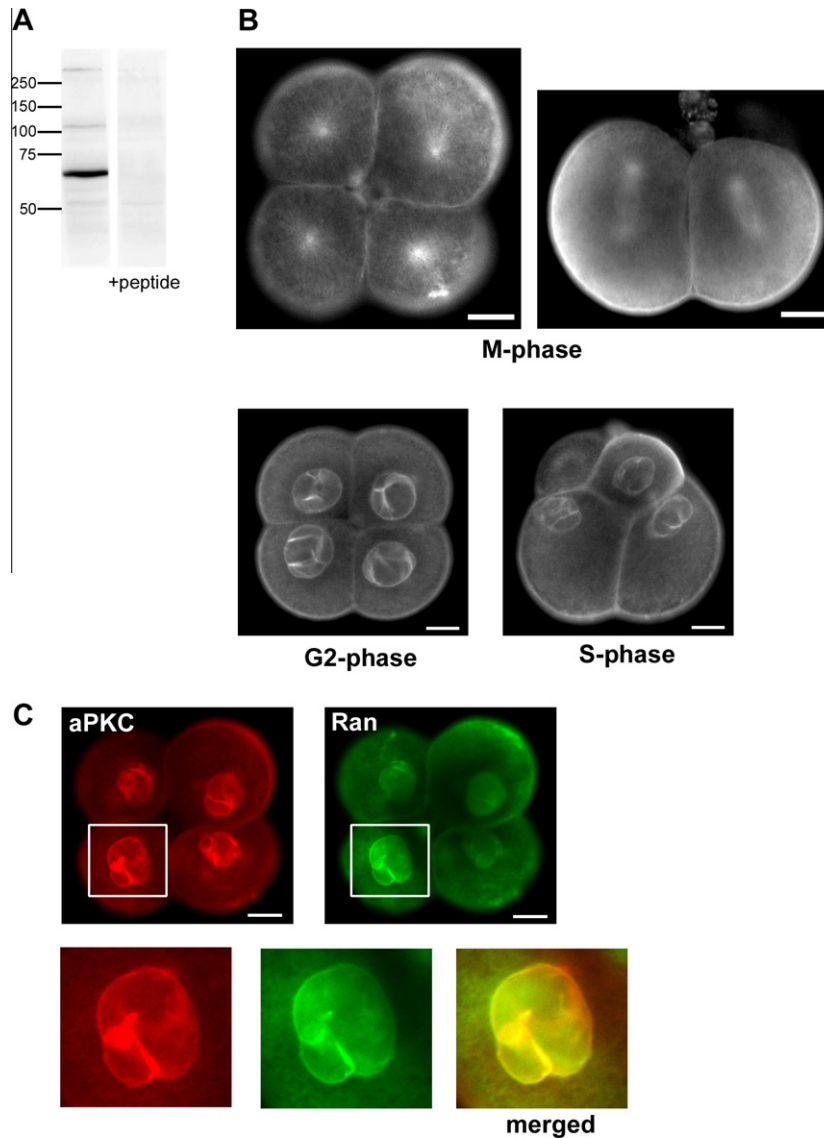


Fig. 4. Characterization of *L. stagnalis* aPKC. (A) Immunoblotting with anti-aPKC. An antibody specific to the conserved C-terminal region of aPKCs was used for the detection of *L. stagnalis* aPKC. The antibody recognized a single band at the expected size of *L. stagnalis* aPKC (69 kDa). The band diminished after adsorption of the antibody with the corresponding antigen peptide. (B, C) Immunofluorescence. Embryos were stained with anti-aPKC antibody alone (B) or double stained with anti-aPKC (red) and anti-Ran (green) antibodies (C). In mitotic embryos, the centrosome and spindle microtubules were visualized by the anti-aPKC antibody. The same antibody labeled the nuclear envelopes (judged from the merged image with the anti-Ran staining) in the S and G2 phases. The antibody gave non-specific cortical staining, which disappeared in the presence of antigen peptide (data not shown). Bars represent 20 μm. (For interpretation of the references in colour in this figure legend, the reader is referred to the web version of this article.)

in the Par system [20], thus LsPar6 may use the second interacting site when the first one is occupied. Alternatively, the tandemly located regions may co-operate, as full-length or full N-terminal LsPar6 consistently yielded higher recovery of tubulin than each of the independent tubulin-binding regions (Fig. 3E). We have also investigated the binding ability of the C-terminal half of LsPar6 by dividing the region into several parts. The C-terminal region (Fig. 3D and E) or any of its fragments (data not shown) showed no tubulin-binding ability. Similar results were obtained in the microtubule-cosedimentation assay (Fig. S3), in which the full-length and N-terminal fragments of LsPar6 exhibited the *in vitro* binding to polymerized microtubules.

In order to test a microtubule modulating activity of LsPar6, a microtubule bundling assay was conducted using recombinant LsPar6 (Fig. 3F). Preassembled microtubules (from X-rhodamine labeled tubulin) were incubated at room temperature with either GST or GST-LsPar6. The reactions were fixed, mounted on slide glasses, and imaged with the confocal microscope. Microtubule

bundling was significantly enhanced with GST-LsPar6 in contrast to buffer or GST alone. This result suggests that the scaffold protein Par6 could modulate microtubules by itself as well as act as a protein hub.

This is the first report to show the direct interaction of Par6 with microtubules. Although Par6 was found to be not the primary determinant of the left–right asymmetry, the direct interaction of Par6 and microtubules implicates that this protein is critically involved in the fixation or stabilization process of spindle orientation, which is relevant in the snail chiromorphology.

3.4. Atypical PKC localizes to the mitotic spindle

Par6 is known to serve as a scaffold protein for the polarity complex. The most frequently tagged partner is aPKC in many systems. We therefore isolated aPKC from *L. stagnalis* and examined its cellular localization (Fig. 4). The isolated cDNA encodes a protein with a molecular weight of 69 kDa (DDBJ ID: AB598833).

The atypical isoforms of PKC have a highly conserved region near the C-terminus and we could detect *L. stagnalis* aPKC with a commercially available antibody specific to this region (Fig. 4A). The immunofluorescence assay revealed aPKC localization on the mitotic spindle (Fig. 4B) with a distribution pattern similar to that of LsPar6. In the S and G2 phases, aPKC was localized in the nuclear envelope (NE), which was confirmed by colocalization with NE-localized Ran GTPase (Fig. 4C). Although LsPar6 was not localized in the NE in the S and G2 phases, the localization pattern observed in the M-phase indicates the possible formation of LsPar6/aPKC complex on the spindle. Persistent interaction between LsPar6 and microtubules throughout the cell cycle implies the recruitment of aPKC on the spindle via the LsPar6/aPKC interaction in the mitotic phase. Investigation on the interaction between *L. stagnalis* Par system (LsPar6-aPKC) and microtubules is currently underway to further reveal the mechanism of this polarity module.

Acknowledgments

We thank Dr. Guss Smit for his generous gift of dextral and sinistral stocks of *L. stagnalis*. We also thank the members of Kuroda Chiromorphology team for their assistance in rearing snails.

Appendix A. Supplementary data

Supplementary data associated with this article can be found, in the online version, at [doi:10.1016/j.bbrc.2010.11.087](https://doi.org/10.1016/j.bbrc.2010.11.087).

References

- [1] J.A. Knoblich, Asymmetric cell division during animal development, *Nat. Rev. Mol. Cell Biol.* 2 (2001) 11–20.
- [2] R. Kuroda, B. Endo, M. Abe, M. Shimizu, Chiral blastomere arrangement dictates zygotic left–right asymmetry pathway in snails, *Nature* 462 (2009) 790–794.
- [3] H. Nishida, Spiral cleavage in gastropod embryos, in: R.A. Pedersen, G.P. Schatten (Eds.), *Current Topics in Developmental Biology*, vol. 46, Academic Press, NY, 1999, pp. 8–10.
- [4] H.E. Crampton, Reversal of cleavage in a sinistral gastropod, *Ann. N. Y. Acad. Sci.* 8 (1894) 167–170.
- [5] G. Freeman, J.W. Lundelius, The developmental genetics of dextrality and sinistrality in the gastropod *Lymnaea peregra*, *Wilhelm Roux Arch. Dev. Biol.* 191 (1982) 69–83.
- [6] J.A.M. van den Biggelaar, P. Guerrier, Origin of spatial organization, in: N.H. Verdonk, J.A.M. van den Biggelaar, A.S. Tompa (Eds.), *The Mollusca Development*, vol. 3, Academic Press, NY, 1983, pp. 179–213.
- [7] Y. Shibasaki, M. Shimizu, R. Kuroda, Body handedness is directed by genetically determined cytoskeletal dynamics in the early embryo, *Curr. Biol.* 14 (2004) 1462–1467.
- [8] E. Munro, J. Nance, J.R. Priess, Cortical flows powered by asymmetrical contraction transport PAR proteins to establish and maintain anterior–posterior polarity in the early *C. elegans* embryo, *Dev. Cell* 7 (2004) 413–424.
- [9] D.J. David, A. Tishkina, T.J. Harris, The PAR complex regulates pulsed actomyosin contractions during amnioserosa apical constriction in *Drosophila*, *Development* 137 (2010) 1645–1655.
- [10] M. Gotta, M.C. Abraham, J. Ahringer, CDC-42 controls early cell polarity and spindle orientation in *C. elegans*, *Curr. Biol.* 11 (2001) 482–488.
- [11] L.M. McCaffrey, I.G. Macara, Widely conserved signaling pathways in the establishment of cell polarity, *Cold Spring Harb. Perspect. Biol.* 1 (2009) a001370.
- [12] A. Suzuki, S. Ohno, The PAR-aPKC system: lessons in polarity, *J. Cell Sci.* 119 (2006) 979–987.
- [13] J.L. Watts, B. Etamad-Moghadam, S. Guo, L. Boyd, B.W. Draper, C.C. Mello, J.R. Priess, K.J. Kemphues, par-6, a gene involved in the establishment of asymmetry in early *C. elegans* embryos, mediates the asymmetric localization of PAR-3, *Development* 122 (1996) 3133–3140.
- [14] J.R. Huynh, M. Petronczki, J.A. Knoblich, D. St. Johnston, Bazooka and PAR-6 are required with PAR-1 for the maintenance of oocyte fate in *Drosophila*, *Curr. Biol.* 11 (2001) 901–906.
- [15] D.C. Bergmann, M. Lee, B. Robertson, M.F. Tsou, L.S. Rose, W.B. Wood, Embryonic handedness choice in *C. elegans* involves the Gα protein GPA-16, *Development* 130 (2003) 5731–5740.
- [16] D.J. Solecki, L. Model, J. Gaetz, T.M. Kapoor, M.E. Hatten, Par6α signaling controls glial-guided neuronal migration, *Nat. Neurosci.* 7 (2004) 1195–1203.
- [17] S. Vinot, T. Le, B. Maro, S. Louvet-Vallée, PAR6 proteins become asymmetrically localized during establishment of polarity in mouse oocytes, *Curr. Biol.* 14 (2004) 520–525.
- [18] M. Abe, M. Shimizu, R. Kuroda, Expression of exogenous fluorescent proteins in early freshwater pond snail embryos, *Dev. Genes. Evol.* 219 (2009) 167–173.
- [19] B. Ozdamar, R. Bose, M. Barrios-Rodiles, H.R. Wang, Y. Zhang, J.L. Wrana, Regulation of the polarity protein Par6 by TGFβ receptors controls epithelial cell plasticity, *Science* 307 (2005) 1603–1609.
- [20] D. Henrique, F. Schweisguth, Cell polarity: the ups and downs of the Par6/aPKC complex, *Curr. Opin. Genet. Dev.* 13 (2003) 341–350.